Draft version March 13, 2019
Typeset using LaTeX default style in AASTeX62

The Empirical Delay Time Distributions of Type Ia Supernovae From Galaxy and Cosmic Star Formation Histories

L.-G. Strolger, Steven Rodney, Camila Pacifici, and et al.

ABSTRACT

blah, blah, blah . . .

1. INTRODUCTION

Understanding cosmic type Ia supernova (SN Ia) rates have a critical importance to understanding galaxy evolutionary feedback mechanisms, the cosmic iron enrichment and α-process element enrichment histories (**?**), and constraining the physical mechanisms of SN Ia progenitors. However, tracing rate histories has been a slog, with the first precise measures of the local ($z \approx 0.0$) rate in the early 1990s (cf. **???**), and the first measures beyond the Hubble flow beginning in the early 2000s as a result of the dark energy experiment (**??**). Since then, there have been several measures of the volumetric SN Ia rate at various redshifts by various groups. These rate values have not always been in total agreement with one another, and there may be several valid reasons as to why (see rev. by Haden?). For the time being it probably best to consider each published rate value as a valid measure. Further, we assume each is valid within their measured statistical error, which again may be bold, but is probably satisfactory given the number of rate measures in each redshift interval. A collection of volumetric SN Ia rates is shown in Figure 1 and in Table 1.

Table 1. Volumetric SN Ia Rates Used in this Work

Redshift	$R_{\rm Ia}$[a]	Stat. Uncertainty	Sys. Uncertainty	Source
0.01	0.28	$^{+0.09}_{-0.09}$	$^{+0.0}_{-0.0}$	**?**
0.03	0.28	$^{+0.11}_{-0.11}$	$^{+0.0}_{-0.0}$	**?**
0.0375	0.278	$^{+0.112}_{-0.083}$	$^{+0.015}_{-0.00}$	**?**
0.1	0.259	$^{+0.052}_{-0.044}$	$^{+0.028}_{-0.001}$	**?**
0.10	0.32	$^{+0.15}_{-0.15}$	$^{+0.0}_{-0.0}$	**?**
0.10	0.55	$^{+0.50}_{-0.29}$	$^{+0.20}_{-0.20}$	**?**
0.11	0.37	$^{+0.10}_{-0.10}$	$^{+0.0}_{-0.0}$	**?**
0.13	0.20	$^{+0.07}_{-0.07}$	$^{+0.05}_{-0.05}$	**?**
0.15	0.307	$^{+0.038}_{-0.034}$	$^{+0.035}_{-0.005}$	**?**
0.15	0.32	$^{+0.23}_{-0.23}$	$^{+0.23}_{-0.06}$	**?**
0.16	0.14	$^{+0.09}_{-0.09}$	$^{+0.06}_{-0.12}$	**?**
0.2	0.348	$^{+0.032}_{-0.030}$	$^{+0.082}_{-0.007}$	**?**
0.20	0.20	$^{+0.08}_{-0.08}$	$^{+0.0}_{-0.0}$	**?**
0.25	0.36	$^{+0.60}_{-0.26}$	$^{+0.12}_{-0.35}$	**?**
0.25	0.365	$^{+0.031}_{-0.028}$	$^{+0.182}_{-0.012}$	**?**
0.25	0.39	$^{+0.13}_{-0.12}$	$^{+0.10}_{-0.10}$	**?**
0.26	0.28	$^{+0.07}_{-0.07}$	$^{+0.06}_{-0.07}$	**?**
0.30	0.34	$^{+0.16}_{-0.15}$	$^{+0.0}_{-0.0}$	**?**
0.30	0.434	$^{+0.037}_{-0.034}$	$^{+0.396}_{-0.016}$	**?**
0.35	0.34	$^{+0.19}_{-0.19}$	$^{+0.19}_{-0.03}$	**?**
0.35	0.36	$^{+0.06}_{-0.06}$	$^{+0.05}_{-0.06}$	**?**
0.42	0.46	$^{+0.42}_{-0.32}$	$^{+0.10}_{-0.13}$	**?**

Table 1 continued on next page

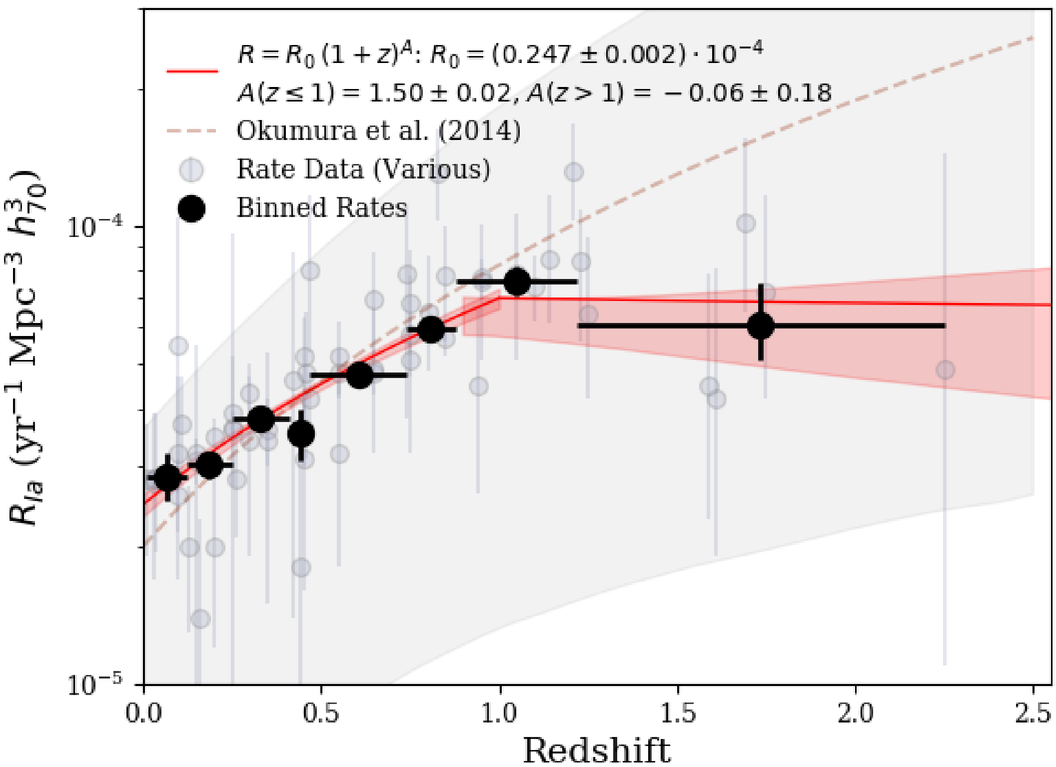

Figure 1. Type Ia supernova volumetric rate measures from various sources in the literature (gray points, see Table 1 for their sources), and binned (black points, see Table 2), largely for illustration. Red lines show a broken power-law fit to the data in redshift space.

Table 1 *(continued)*

Redshift	$R_{\rm Ia}$ [a]	Stat. Uncertainty	Sys. Uncertainty	Source
0.44	0.262	$^{+0.229}_{-0.133}$	$^{+0.059}_{-0.120}$	?
0.45	0.31	$^{+0.15}_{-0.15}$	$^{+0.15}_{-0.04}$	?
0.45	0.36	$^{+0.06}_{-0.06}$	$^{+0.04}_{-0.05}$	?
0.45	0.52	$^{+0.11}_{-0.13}$	$^{+0.16}_{-0.16}$	?
0.46	0.48	$^{+0.17}_{-0.17}$	$^{+0.0}_{-0.0}$	?
0.47	0.42	$^{+0.06}_{-0.06}$	$^{+0.13}_{-0.09}$	?
0.47	0.80	$^{+0.37}_{-0.27}$	$^{+1.66}_{-0.26}$	?
0.55	0.32	$^{+0.14}_{-0.14}$	$^{+0.14}_{-0.07}$	?
0.55	0.48	$^{+0.06}_{-0.06}$	$^{+0.04}_{-0.05}$	?
0.55	0.52	$^{+0.10}_{-0.09}$	$^{+0.0}_{-0.0}$	?
0.65	0.48	$^{+0.05}_{-0.05}$	$^{+0.04}_{-0.06}$	?
0.65	0.49	$^{+0.17}_{-0.17}$	$^{+0.17}_{-0.08}$	?
0.65	0.69	$^{+0.19}_{-0.18}$	$^{+0.27}_{-0.27}$	?
0.74	0.79	$^{+0.33}_{-0.41}$	$^{+0.0}_{-0.0}$	?
0.75	0.51	$^{+0.27}_{-0.19}$	$^{+0.23}_{-0.19}$	?

Table 1 continued on next page

Table 1 *(continued)*

Redshift	$R_{\rm Ia}$[a]	Stat. Uncertainty	Sys. Uncertainty	Source
0.75	0.58	$^{+0.06}_{-0.06}$	$^{+0.05}_{-0.07}$	?
0.75	0.68	$^{+0.21}_{-0.21}$	$^{+0.21}_{-0.14}$	?
0.80	0.839	$^{+0.230}_{-0.185}$	$^{+0.060}_{-0.120}$	?
0.83	1.30	$^{+0.33}_{-0.27}$	$^{+0.73}_{-0.51}$	?
0.85	0.57	$^{+0.05}_{-0.05}$	$^{+0.06}_{-0.07}$	?
0.85	0.78	$^{+0.22}_{-0.22}$	$^{+0.22}_{-0.16}$	?
0.94	0.45	$^{+0.22}_{-0.19}$	$^{+0.13}_{-0.06}$	?
0.95	0.76	$^{+0.25}_{-0.25}$	$^{+0.25}_{-0.26}$	?
0.95	0.77	$^{+0.08}_{-0.08}$	$^{+0.10}_{-0.12}$	?
1.05	0.79	$^{+0.28}_{-0.28}$	$^{+0.28}_{-0.41}$	?
1.1	0.74	$^{+0.12}_{-0.12}$	$^{+0.10}_{-0.13}$	?
1.14	0.705	$^{+0.239}_{-0.183}$	$^{+0.102}_{-0.103}$	?
1.21	1.32	$^{+0.36}_{-0.29}$	$^{+0.38}_{-0.32}$	?
1.23	0.84	$^{+0.25}_{-0.28}$	$^{+0.0}_{-0.0}$	?
1.25	0.64	$^{+0.31}_{-0.22}$	$^{+0.34}_{-0.23}$	?
1.59	0.45	$^{+0.34}_{-0.22}$	$^{+0.05}_{-0.09}$	?
1.61	0.42	$^{+0.39}_{-0.23}$	$^{+0.19}_{-0.14}$	?
1.69	1.02	$^{+0.54}_{-0.37}$	$^{+0.0}_{-0.0}$	?
1.75	0.72	$^{+0.45}_{-0.30}$	$^{+0.50}_{-0.28}$	?
2.25	0.49	$^{+0.95}_{-0.38}$	$^{+0.45}_{-0.24}$	?

^{a}In units 10^{-4} yr^{-1} Mpc^{-3} h^3_{70}

Table 2. Binned volumetric SN Ia rates, with statistical uncertainties.

Redshift	$R_{\rm Ia}$[a]
0.07 ± 0.06	$0.28^{+0.04}_{-0.03}$
0.19 ± 0.06	$0.30^{+0.02}_{-0.02}$
0.33 ± 0.08	$0.38^{+0.02}_{-0.02}$
0.44 ± 0.03	$0.35^{+0.05}_{-0.04}$
0.61 ± 0.14	$0.47^{+0.03}_{-0.03}$
0.81 ± 0.07	$0.60^{+0.04}_{-0.04}$
1.05 ± 0.17	$0.76^{+0.06}_{-0.06}$
1.73 ± 0.52	$0.61^{+0.14}_{-0.10}$

^{a}In units 10^{-4} yr^{-1} Mpc^{-3} h^3_{70}

It would be reasonable to assume the volumetric rates follow a broken power law evolution with redshift, i.e., $R_{Ia} = R_0\,(1+z)^A$ where at $z < 1$ the power-law slope is $A = 1.50 \pm 0.02$ (with $R_0 = 2.47 \pm 0.02 \times 10^{-5}$ yr^{-1} Mpc^{-3} h^3_{70}), which flattens substantially to $A = -0.06 \pm 0.2$ at redshifts greater than 1, as is shown in Figure 1. This is broadly consistent with the power-law fit of ?, and the locus with the measured SN Ia rate at $z \approx 0$ from ? of approximately $2.7 \pm 0.3 \times 10^{-5}$ yr^{-1}.

2. DELAY TIME DISTRIBUTIONS FROM VOLUMETRIC SN IA RATES AND THE COSMIC STAR FORMATION HISTORY

For these types of analyses, the standard assumption is that the stellar death rate (or supernova rate) is related to the stellar birth rate, convolved with some delay-time distribution that contains all the temporal factors of stellar evolution (e.g., main sequence lifetime, etc.) and binary star evolution (e.g., accretion rates or merger times). Two additional terms include the fraction of the initial mass function (or IMF) that are the progenitors to the SNe Ia (presumably $3-8\,\mathrm{M}_\odot$ zero-age main sequence stars, see discussion in Section 2.1), and the fraction of that population that are actually capable of producing events, as not are necessarily in the right type of binary system or systems.

We can relate volumetric SN Ia rate history to the cosmic star formation history($\dot{\rho}_\star$) in a similar way, expressed mathematically by,

$$R_{\mathrm{Ia}}(t) = h^2\, k\, \varepsilon \left[\dot{\rho}_\star(t) * \Phi(t)\right], \tag{1}$$

where $\Phi(t)$ is the delay-time distribution of SNe Ia, k is the fraction of the IMF (by mass) responsible for SN Ia progenitors, ε is the fraction of that population that are ultimately successful in producing SNe Ia, and t is the forward-moving clock of the universe.

2.1. *The Fraction of Stars Responsible for SNe Ia*

Dissecting each of these terms, k is perhaps the easiest to approximate. The progenitors of SNe Ia have traditionally been CO WD which acquire sufficient mass to approach or exceed the Chandrasekhar mass limit, $M_{ch} = 1.44\,M_\odot$. To only marginally achieve this, they can either start at sufficiently high mass to require only a small amount of accretion from a nearby companion (typically single-degenerate, or SD, scenarios), or as a pair of WD that have combined in mass to meet this criterion (the double-degenerate, or DD, scenario) setting an even lower constraint (see **?**, for a review). In the case of WD/WD mergers, WD mass distributions are strongly peaked around $M_{\mathrm{WD}} \approx 0.6 \pm 0.1\,M_\odot$ (**?**), in which a pair drawn from such distribution may be satisfactorily close to the ignition threshold of a carbon core for a non-rotating CO WD, approximately $1.38\,M_\odot$ (**??**). Initial-Final Mass relations (e.g., **??**) would correspond these to ZAMS masses of approximately $3\,M_\odot$, but no less than $\sim 2.5\,M_\odot$.

The same Initial-Final Mass relations would suggest that a WD essentially at M_{ch} would fall just below $8\,M_\odot$ ZAMS. On a more physical bases, simulations show that the lowest mass in which C ignition is still possible is around $6-8\,M_\odot$ **??**, but likely no more than $\sim 11\,M_\odot$ (**?**), above which an electron-capture-induced collapse mechanism begins, marking the onset of core-collapse supernovae.

It is reasonable, therefore, to assume a progenitor mass range of about $3-8\,M_\odot$ ZAMS. From a numerical assessment of these stars, assuming they fall within an IMF that is a power-law distribution by mass (in this initial mass range) with $\alpha \approx -2.3$ (**??**), one would expect

$$k = \frac{\int_{3M_\odot}^{8M_\odot} \xi(M)\, dM}{\int_{0.1M_\odot}^{125M_\odot} M\, \xi(M)\, dM}, \tag{2}$$

where $k = 0.021^{+33\%}_{-24\%}\, M_\odot^{-1}$. The error in k is driven more by choices in the upper and lower value in the selected mass range of SN Ia progenitors than by the choice in IMF model, as described above.

The fraction of CO WDs that are successful in making SNe Ia is hard to determine, as we don't quite yet know the details of the progenitor mechanism or mechanisms. Estimates swing rather wildly from (perhaps) from as low as 1 in 200 (**?**) to as optimistic as 1 in 40 (**?**). There is at least strong consensus that accretion on to a CO WD is essential, but very different plausible WD close binary scenarios from at least a theoretical standpoint (**??**). The binary fractions of WDs has been recently estimated from the the ESO-VLT Supernova-Ia Progenitor Survey (**?**, SPY) show close double WD systems may have $\varepsilon_{\mathrm{bin}} \simeq 0.1 \pm 0.02$, with separations distributed following a power-law slope of $\alpha = -1.3 \pm 15\%$ (**?**). It is not likely all of these successfully yield SNe Ia as their merger rates in the MW are at least a magnitude higher than best estimates of the SN Ia rate in our galaxy, and presumably some of these will form AM CVn and R Corona Borealis stars, but at least it could be treated as an upper limit on ε.

2.2. *The star-formation density history*

The cosmic star formation history (CSFH), at least to $z < 5$, or over 90% of the history of the universe, is fairly well understood, with (**?**, MD14 hereafter) providing one of the most complete compilations. More recently, the CSFH derived from the combined GAMA, G10-COSMOS, and 3D-HST datasets by **?**, in a quasi-homogeneous analysis over a larger area, provides a dataset with greatly reduced uncertainties per datum, but fewer data than cited in the MD14

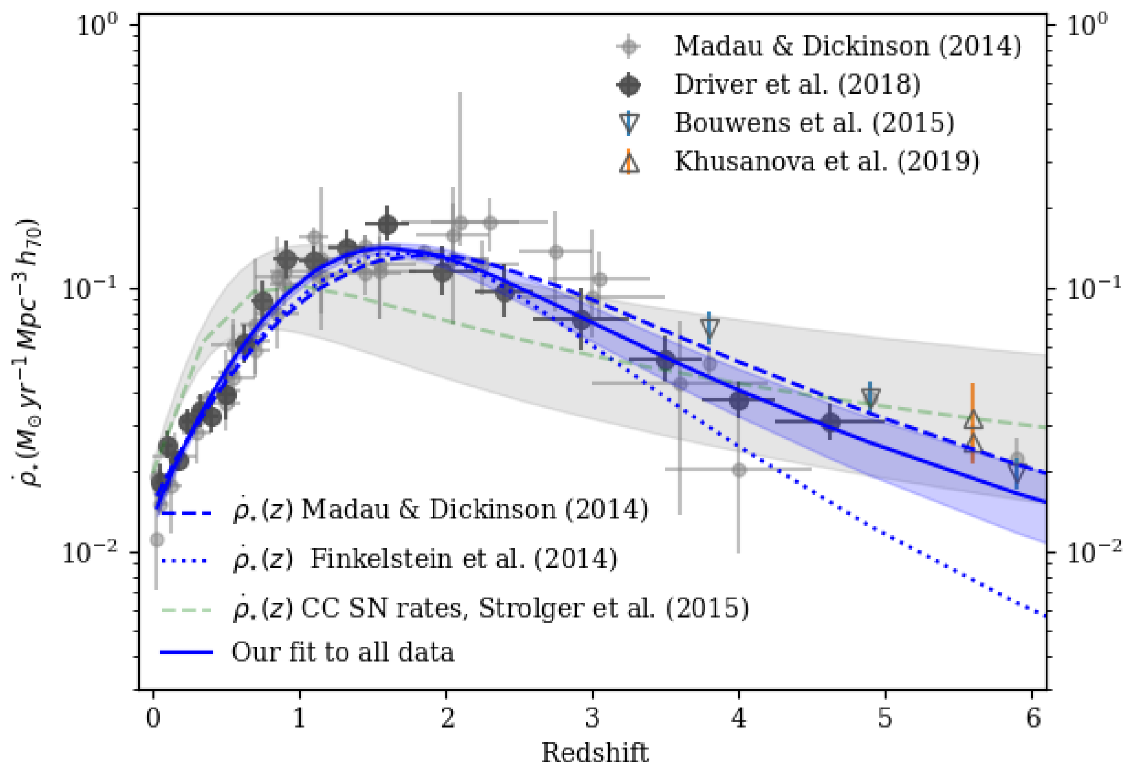

Figure 2. Shown are a compendium of cosmic star formation histories, from **?**, **?**, **?**, and **?**. Dashed lines (and associated shaded regions) are previous models from **?**, **?**, **?**, as indicated. Solid blue line (and blue shaded region) represent our best-fit model to the compendium of data.

compendium (see Figure 2). We combine the MD14 and **?** data, with additional star-formation rate densities from **?** and **?**, to arrive at today's compendium CSFH using the parameterization,

$$\dot{\rho}_\star(z) = \frac{A\,(1+z)^C}{((1+z)/B)^D + 1}. \tag{3}$$

We first correct the **?** data for dust attenuation following the prescription in MD14, by applying

$$\dot{\rho}_\star(z) = h^3 \left[1 + 10^{0.4 \cdot A_{\rm FUV}(z)}\right] \dot{\rho}_{\star,\rm uncorrected}(z), \tag{4}$$

where it is assumed $A_{\rm FUV}(z)$ has essentially the same functional form of Equation 3, and when applied to the MD14 $A_{\rm FUV}(z)$ data results in a Levenberg-Marquardt least-squares solution of $A = 1.4 \pm 0.1$, $B = 3.5 \pm 0.4$, $C = 0.7 \pm 0.2$, and $D = 4.3 \pm 0.7$. We then fit Equation 3 to the combined CSFH datasets, resulting in parameters which are shown in Table 3 and Figure 2.

Table 3. Cosmic Star Formation History Parameter Fits

	A	B	C	D
? only	0.013 ± 0.001	2.6 ± 0.1	3.2 ± 0.2	6.1 ± 0.2
? only	0.014 ± 0.001	2.5 ± 0.2	3.3 ± 0.3	6.2 ± 0.3
All Combined Data	0.0134 ± 0.0009	2.55 ± 0.09	3.3 ± 0.2	6.1 ± 0.2

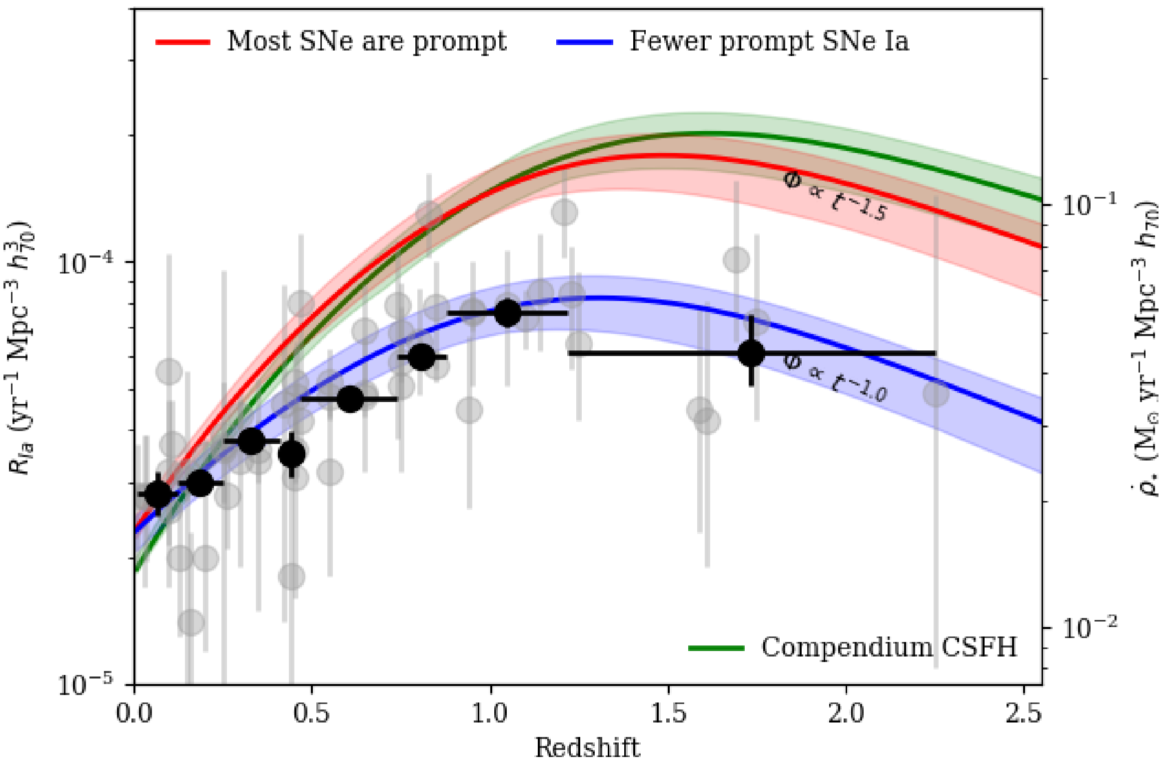

Figure 3. Shown in comparison to the data are the expected volumetric rates for power-law delay-time distributions ($\alpha = 1.0$ and 1.5 in red and blue, respectively) as applied to the cosmic star formation rates (**??**, in solid and dashed green, respectively). Dashed rate models require a higher fraction of WD progenitors than the solid lines.

2.3. *SN Ia Progenitor Delay-Time Distribution Models*

[NOTE: talk about the expected delay-time distribution, values from Graur and Maoz, inability to probe turnover at 'SN high noon', around $z \sim 1$.]

Following **?**, we can continue to test a robust delay-time model, capable of reproducing the theoretical distributions for SD and DD models at one extreme, and δ-function delay times at the other. The unimodal, skew-normal $\Phi(\tau)$ function is defined as:

$$\Phi(\tau) = \frac{1}{\omega\pi} \exp\left(\frac{-(\tau-\xi)^2}{2\omega^2}\right) \int_{-\infty}^{\alpha\left(\frac{\tau-\xi}{\omega}\right)} \exp\left(\frac{-t'^2}{2}\right) dt', \tag{5}$$

where location (ξ),[1] width (ω^2), and shape (α) are defined by the model. Figure 4 demonstrates the flexibility of the model in producing various distributions in τ.

Figure 4 demonstrates the flexibility of the model in producing various distributions in τ.

2.4. *The Optimized Solution*

We apply a maximum likelihood estimation method to determine the best-fit unimodal delay time model to Equation 1 using a method described in **?** and the `emcee.py` documentation (**?**). We assume, for simplicity, that the errors of all survey data are gaussian in nature, but may be underestimated by some factor (f), which may be correctly justified given we are only using the statistical error produced for each value. As follows, we adopt the likelihood

[1] Different from the initial mass function, $\xi(M)$.

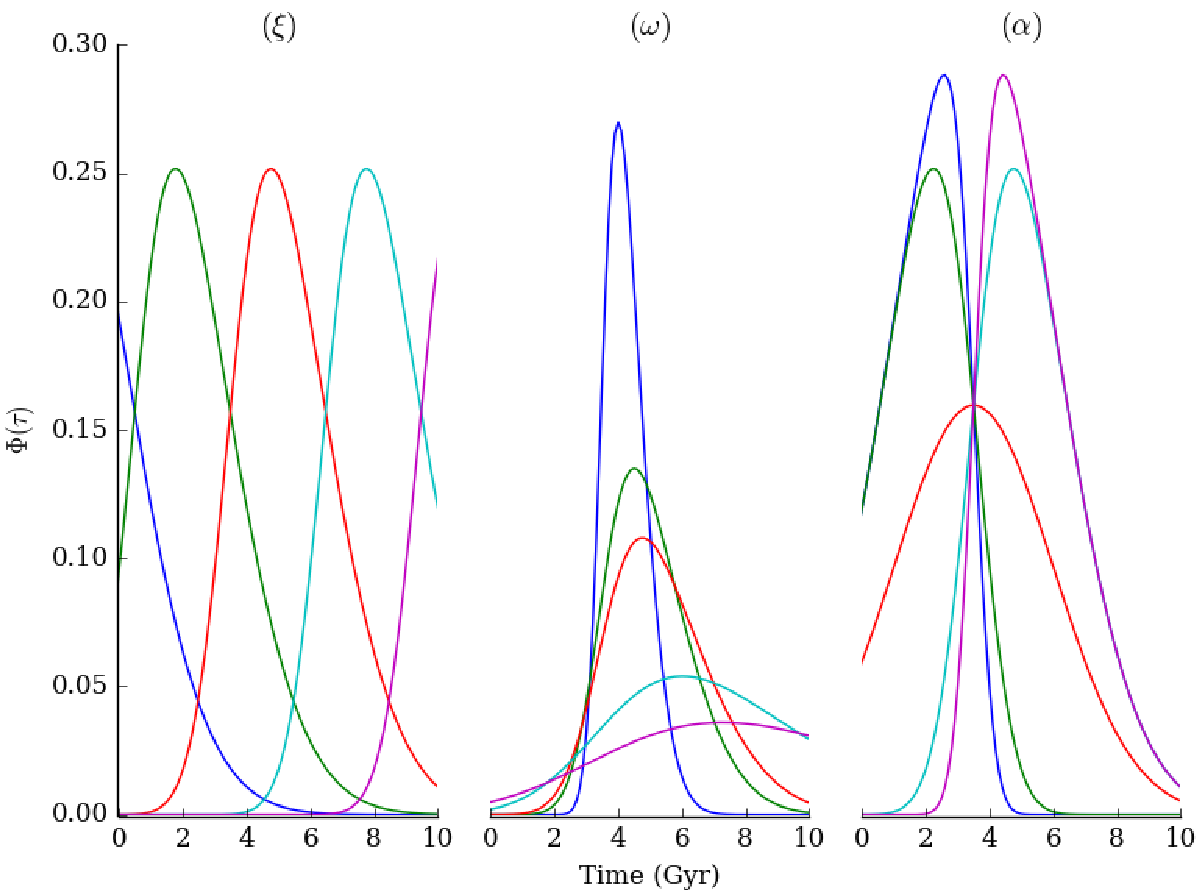

Figure 4. Families of delay-time distributions models shown for various values of location (ξ) fixing other parameters (left plot of figure), width (ω, middle plot), and shape (α, right plot), for illustration purposes.

Table 4. Results for unimodal model

Model test	ε	ξ	ω	α	$\ln f$
CSFH Max. Likelihood	0.062	-1669.7	69.1	88.7	-2.99
CSFH MCMC	$0.058^{+0.003}_{-0.007}$	-1090^{+1050}_{-650}	54^{+15}_{-40}	202^{+203}_{-198}	$-2.5^{+1.5}_{-0.9}$

function to be:

$$\ln p(y|x,\sigma,\varepsilon,\xi,\omega,\alpha,f) = -\frac{1}{2}\sum_i \left\{ \frac{[R_{\mathrm{Ia},i} - \mathrm{model}(t_i;\varepsilon,\xi,\omega,\alpha)]^2}{s_i^2} + \ln(2\pi s_i^2) \right\}, \tag{6}$$

where,

$$s_i^2 = \sigma_i^2 + f^2\,\mathrm{model}(t_i;\varepsilon,\xi,\omega,\alpha)^2. \tag{7}$$

We then find the optimal parameters which maximize this likelihood. As for priors, we require the successful fraction of progenitors to be between zero and 1 ($0 < \varepsilon < 1$), that the width parameters can only be positive ($\omega > 0$), and the that underestimation fraction can only be between approximately zero and 1 ($-4 < \ln f < 0$). Otherwise, we apply rather loose and arbitrarty bounds of $-2000 < \xi < 2000$ and $-500 < \alpha < 500$. The results of this fit are shown in Figure 5, and in Table 4.

While the optimization results in values with associated errors, that are broadly consistent with the t^{-1} model, it is not directly possible to estimate the range of validity in this maximum likelihood optimization method. A Markov chain Monte Carlo (MCMC) is better suited for that.

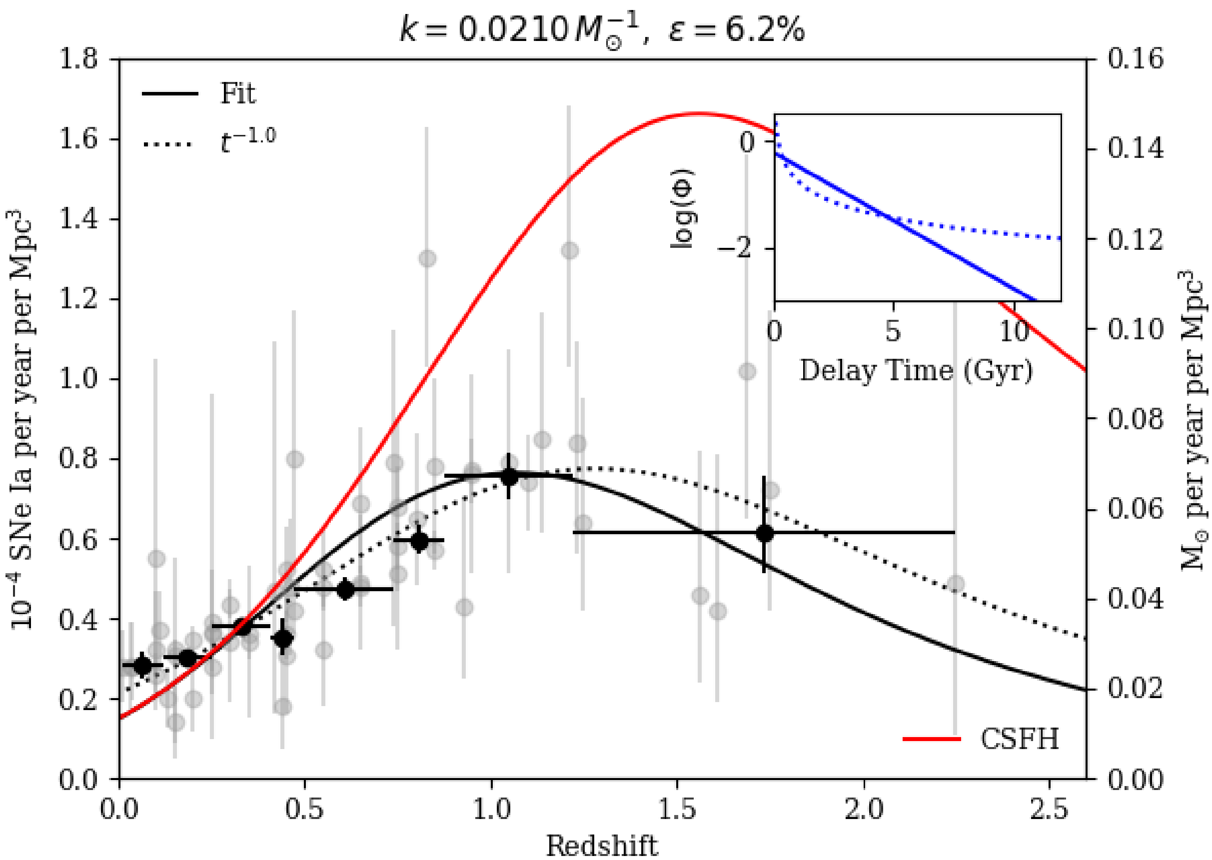

Figure 5. In addition to rate values shown in previous figures, the $R_{\rm Ia}(z)$ result of from optimal parameter fitting is show (black line). The CSFH is shown on in red, and along the secondary abscissa.

2.5. *The MCMC solution*

Exploring the parameter space in an MCMC allows both confirmation of the optimized solution and an exploration of the range of validity. We use the affine-invariant MCMC ensemble sampler from `emcee.py` (?) using the same likelihood function as shown in Equation 6, and set our uniform priors as described by the bounds, as shown in the previous section, with the exception of evaluating $\ln \varepsilon$ to allow MCMC step sizes of order unity, and using the prior $-10 < \ln \varepsilon < 0$. We then set 1,000 walkers to explore 10,000 steps, for a total of 10 million iterations, the first 100,000 of which we discard as 'burn-in'. The results of which are shown in Figure 9 and Table 4.

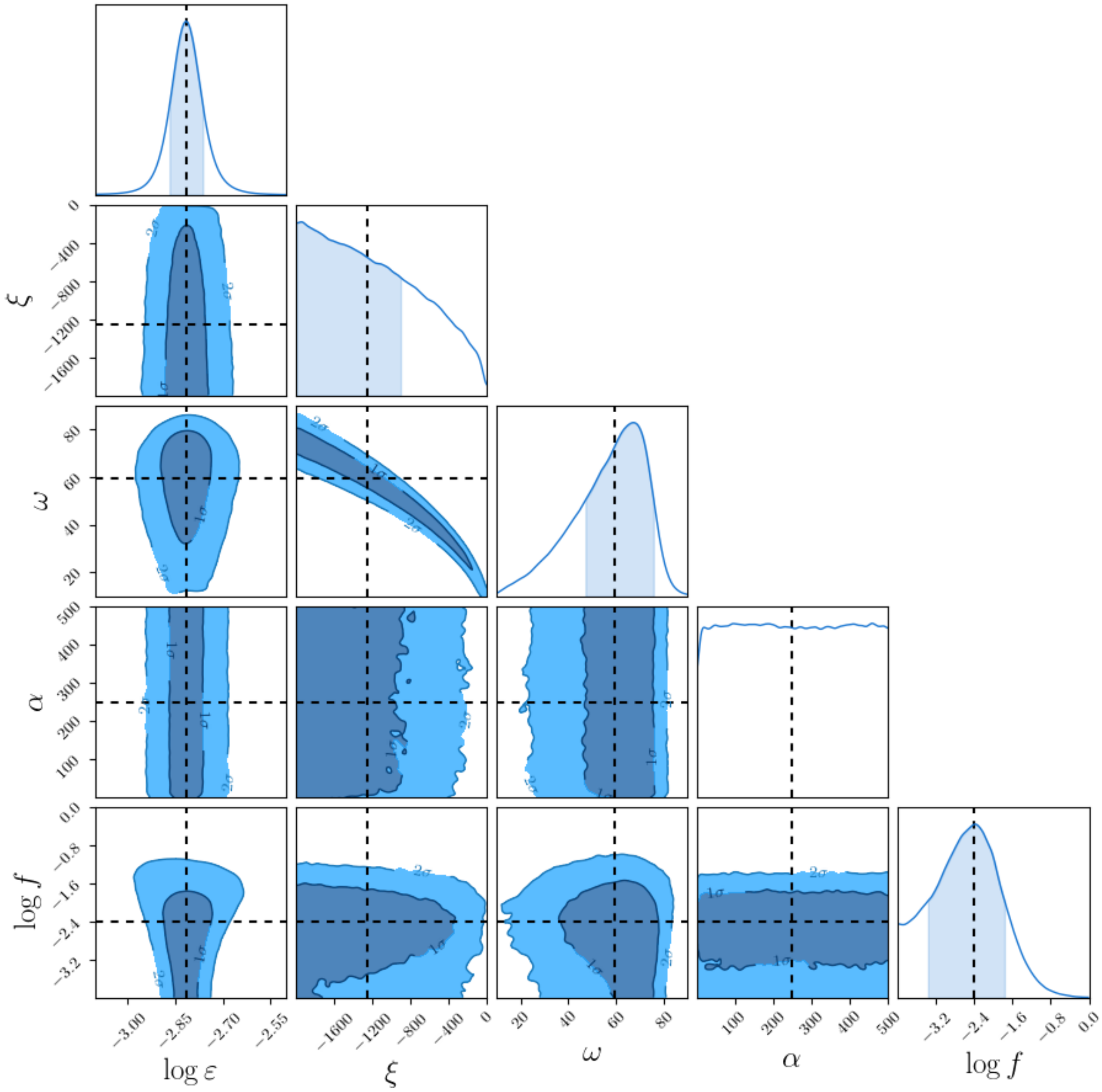

Figure 6. MCMC results on unimodal delay-time distribution model, fit to volumetric rate data and CSFH. Plot generated using `ChainConsumer.py` (?).

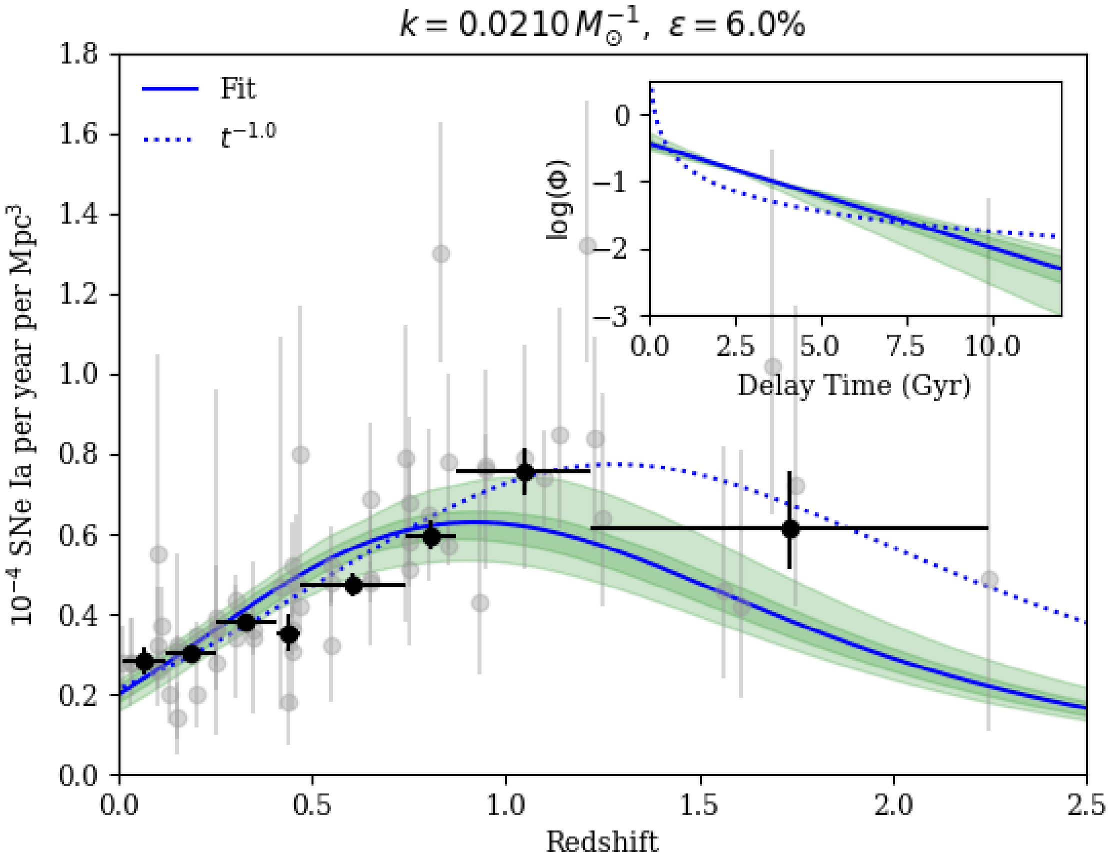

Figure 7. Similar to Figure 5, the $R_{\rm Ia}(z)$ result of from MCMC fitting is shown (blue line), with the 68% confidence interval, in green.

As these result show, there is a clear convergence in $\ln f$, the factor by which reported errors in rate measures are underestimated. It seems that nearly all values are underestimated by less than 37%, with most only about 8% underestimated. While there is a large dispersion in rate values, and seemingly inconsistent rates in some of the same redshift ranges, their values are reasonably consistent with statistical errors, which are not grossly underestimated. Also fairly well constrained is the fraction ε, where only $5.8^{+0.3}_{-0.7}\%$ of WD stars contribute as SN Ia progenitors. However, the parameters we wished to know the most about, ξ, ω, and α, appear very much less constrained by the MCMC. There is a clear peak around $\omega \approx 60$, but that value is also highly degenerate with the value of ξ. There does not appear to be any convergence or preference in the value of α.

While this does not seem to show a clear preference for a very specific parameterization the model, it does indicate a specific family of solutions that are related. As shown in Figure 7, the 68% confidence interval about the best fit parameters, all indicate a rather flat DTD.

[NOTE: I should at least talk about Parallel-Tempering Ensemble MCMC, and ...]

3. DELAY TIME DISTRIBUTIONS FROM STAR FORMATION HISTORIES

This is an evaluation of the maximum likelihood delay time distribution following the prescription of **?** but performed on the GOODS/CANDELS galaxies.

For this analysis we use star formation histories derived using the modeling approach of **?**. In summary, the galaxy physical propertes (including star formation histories) are retrieved from a combined analysis of stellar and nebular emission, utilizing an extensive library of star formation and chemical enrichment histories to build a large library of galaxy spectral energy distributions, then determining likelihood distributions of physical parameters from a Bayesian analysis of observed spectral energy distribtions. This is method has been applied to the HST/WFC3-F160W-selected

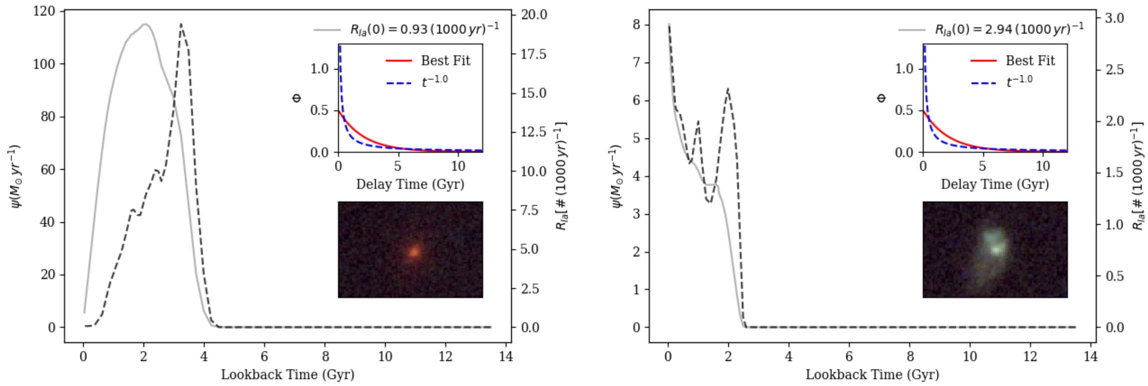

Figure 8. Example star formation histories (dashed-line and left abcisa), and the resultant SN Ia rate histories (dotted-line and right abcisa) for two SN Ia host galaxies in our sample, SN 2002hp (left) and 2003dy (right), in the GOODS-South and GOODS-North fields, respectively. Insets show the delay time disribution applied (upper right, in red) compared to t^{-1} (blue dashed), and a three-color HST ACS/WFC image (lower right) of the SN host galaxy.

CANDELS catalogs for the GOODS-South (Guo et al. 2013), and the GOODS-North (Barro et al. , in preparation), into SFH catalogs **?**. We adopt only the median derrived SFH of each galaxy for simplicity.

For a given galaxy, the rate history of SNe Ia per year (r_i) would be:

$$r_i(t) = h^2\,k\,\varepsilon \int_0^t \Psi_i(t')\,\Phi(\tau - t')\,dt', \tag{8}$$

where Ψ_i is the star formation history of the galaxy (mapped in look-forward time), and Φ is the global delay time distribution model, also in look-forward time. Figure 8 shows an example "SN Ia rate history" one would derive from Equation 8 using the best-fit model from the MCMC on CSFHs, done in the previous sections.

The product of the rate at the observed epoch ($r_{i,0}$) and the observed control time ($t'_{c,i}$) of the galaxy– which contains all the information on the temporal sampling and depth of the survey– give (m_i) the expected number of observed SN Ia events over the duration of the survey, or

$$m_i = r_i\,t'_{c,i}. \tag{9}$$

The probability distribution of those observed events is likely Poisson, where of catching n_i SNe Ia from that galaxy when m_i are expected is

$$P(n_i|m_i) = \frac{m_i^{n_i} e^{-m_i}}{n_i!}. \tag{10}$$

The product of probabilities for all galaxies in the survey would then serve as the likelihood of a given delay-time distribution model. The log-likelihood, convenient for MCMCs, is then expressed by:

$$L = \prod_i^N P(n_i|M_i) \Rightarrow \ln L = -\sum^N m_i + \sum^N \ln\left(\frac{m_i^{n_i}}{n_i!}\right) \tag{11}$$

in which the last term is zero for the galaxies which did not host SNe Ia during the survey.

Examples of this method are shown in Figure 8 which shows star-formation histories for two SN Ia host galaxies, for SN 2002hp and SN 2003dy, respectively (see **?** for futher details on these events). Both events are at $z \approx 1.3$, and in the GOODS-South and GOODS-North fields, respectively. The host of SN 2002hp however is a passive galaxy that underwent a very large burst of star formation just a few Gyr ago, that when convolved with the applied delay time distribution results in a realtively large rate of SN Ia at the observed epoch of 0.93 per millineum. Conversely, the host of SN 2003dy is actively star forming and has been over the last few Gyr, resulting in a SN Ia rate at the observed epoch about three times larger, 2.94 per millenium. Most non-hosts have predicted SN Ia rates at their observed epochs several orders of magnitude smaller than these two example hosts.

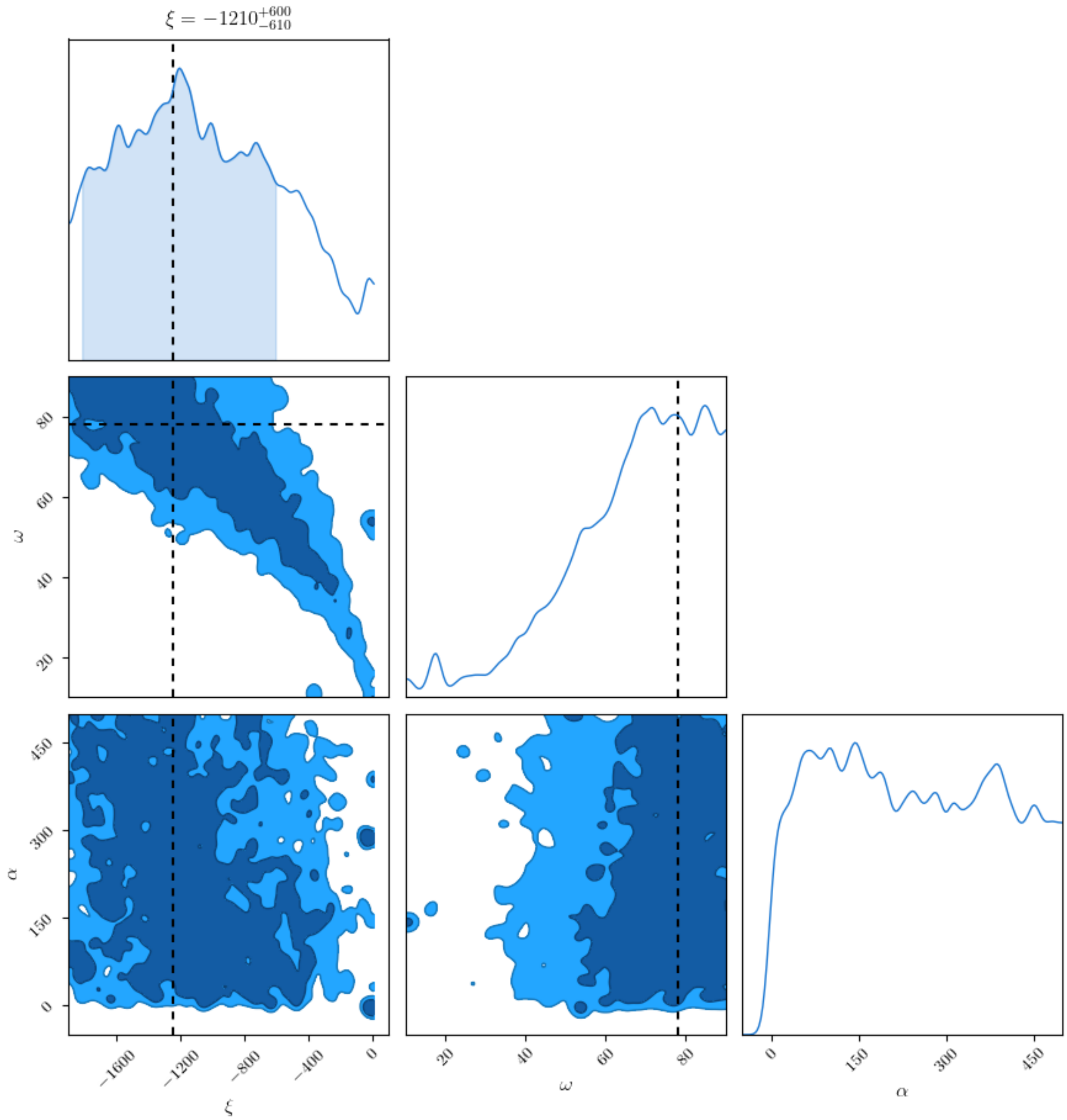

Figure 9. MCMC results on unimodal delay-time distribution model, fit to SFHs for 147 galaxies in CANDELS, 49 of which are SN Ia hosts.

There are 34 events we classified in **???** as SNe Ia in the GOODS/CANDELS South field, and 39 in the North field, all but 6 of which were matched to a host galaxy in the SFH catalog. Two were rejected as the host redshifts were inconsistent with the catalog redshifts, and the other 4 were rejected as they were not in the catalog, largely as they were either too faint or near the field edge to be listed in their composite photometry catalogs.

The model parameters, ξ, ω, and α is then explorable via `emcee.py`. We keep the same uniform priors as bounds, as described in Sections 2.4 and 2.5.

4. DISCUSSION

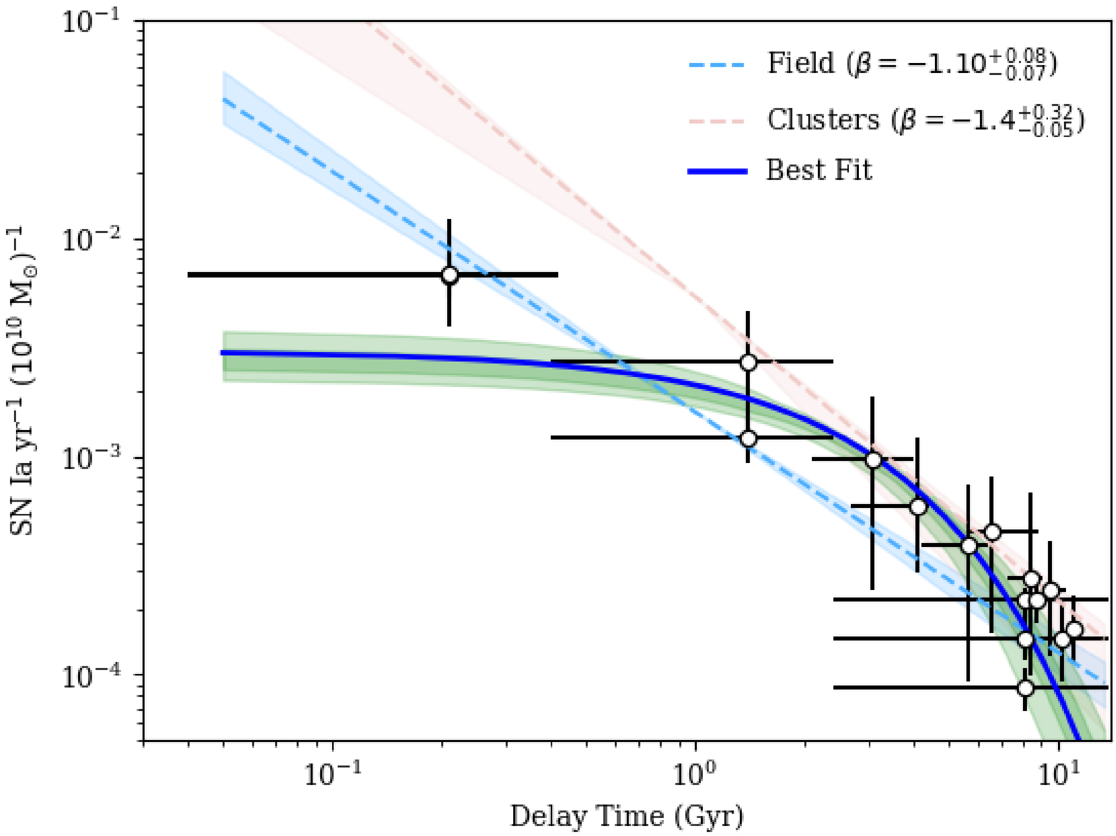

Figure 10. temp

Table 5. Parameter Covariance MCMC SFD

	f	ξ	ω	α	$\log \phi$
f	0.41	-125.69	6.61	33.98	-0.41
ξ	-125.69	412816.10	-14898.10	-52398.20	518.74
ω	6.61	-14898.10	660.60	2209.32	-22.89
α	33.98	-52398.20	2209.32	27290.24	-131.67
$\log \phi$	-0.41	518.74	-22.89	-131.67	2.35